JOURNAL OF GEOPHYSICAL RESEARCH, VOL. 104, NO. D3, PAGES 3605–3620, FEBRUARY 20, 1999

Findings on NO_y as an indicator for ozone sensitivity based on different numerical simulations

B. Vogel, N. Riemer, H. Vogel, and F. Fiedler

Institut für Meteorologie und Klimaforschung, Forschungszentrum Karlsruhe/Universität Karlsruhe, Karlsruhe, Germany

Abstract. The O_3-NO_y relation for a polluted planetary boundary layer is investigated using numerical simulations and observations. Box model runs are carried out to study the sensitivity of the transition value of NO_y, which separates the low-NO_x and the high-NO_x regimes, to changes in emissions and in ambient conditions. It is shown that the transition value of NO_y depends on the hydrocarbon and NO_x emissions, on water vapor, on radiation, and on temperature. Increasing hydrocarbon emissions, increasing water vapor, increasing radiation, or increasing temperature shifts the transition value to higher levels. One-dimensional simulations, which include vertical mixing and dry deposition, show that increasing dry deposition reduces the transition value of NO_y. Sensitivity studies with a three-dimensional nonhydrostatic model system are carried out to investigate the effects of transport. A smoothing procedure is applied to reduce the large scatter of the O_3-NO_y relation which is found in these cases. After smoothing, a transition value can be identified. For the southwestern part of Germany it is shown that this transition value indicates areas where NO_x reduction leads to the most effective ozone reduction. Runs with various scenarios show the dependence of the transition value on emissions and ambient conditions. A normalization procedure is introduced. The normalization procedure is applied to the model results and to observations. Under high-NO_x conditions a large difference between the cases with and without advection is found. It shows that in the three-dimensional case the ozone concentration is less sensitive to changes in the NO_x emissions than in the case of pure chemistry.

1. Introduction

High ozone values during the summer months are still the main air pollution problem in industrialized areas with high population density. Ozone formation in the troposphere shows a nonlinear dependence on the availability of the precursors nitrogen oxides (NO_x = NO + NO_2) and volatile organic compounds (VOCs). In the real atmosphere, physical processes such as advection, turbulent diffusion, and dry deposition make the situation even more complex [*McKeen et al.*, 1991a]. Temperature, humidity, and radiation, the latter determining the photolysis rate coefficient, have a direct influence on ozone chemistry [*Cardelino and Chameides*, 1990; *Sillman and Samson*, 1995; *Vogel et al.*, 1995]. Anthropogenic and biogenic emissions of the precursors of ozone vary in space and time. For these reasons, simply using the ratio of the emissions of NO_x and VOCs is not sufficient when studying the sensitivity of ozone production [*Sillman*, 1995a].

Much progress has been made during the last decades in understanding the basic physical and chemical processes which lead to enhanced ozone concentrations. However, the nonlinearity of photochemistry raises a number of difficulties. Therefore the problem of deriving effective abatement strategies is still unsolved [*National Research Council (NRC)*, 1991].

Milford et al. [1994] have proposed NO_y (NO_y = NO + NO_2 + HNO_3 + PAN + ···) as an indicator to identify areas which would benefit from reduction of NO_x emissions and areas where a reduction of VOC emissions leads to decreasing ozone concentrations. For this purpose, transition values for NO_y were calculated using the results of different numerical models. *Milford et al.* [1994] found a substantial uncertainty in the transition value of NO_y (10 to 25 ppb). *Sillman* [1995b] introduced additional indicators such as H_2O_2 and HNO_3. Later on, the concept of indicators was applied with different numerical models. *Staffelbach and Neftel* [1997] used a trajectory model to study the photochemical oxidant production over southern Switzerland. They compared their modeled concentrations of the indicators with observations [*Staffelbach et al.*, 1997] and used the transition values of *Sillman* [1995b] (20 ppb in the case of NO_y) to define whether the ozone formation is NO_x sensitive or whether it is VOC sensitive. *Vogel et al.* [1996a] studied the NO_x sensitivity of the ozone formation in the area of Baden-Württemberg, Germany. They used the comprehensive three-dimensional model system KAMM/DRAIS [*Vogel et al.*, 1995] and observations which were carried out during the Transport of Pollutants Over Complex Terrain (TRACT) campaign [*Zimmermann*, 1995]. A transition value for NO_y (10 ppb) was found that differs from *Sillman*'s [1995b] value. *Andreani-Aksoyoglu and Keller* [1997] looked for transition values of indicators for the area of Switzerland. They applied the Urban Airshed Model [*Morris and Myers*, 1990] and found that the transition values of the indicators depend on the wind conditions. *Lu and Chang* [1997] used the SARMAP air quality model to test the indicator approach for the San Joacquin Valley, California. From the fact that the transition values for the indicators are different from those of *Sillman* [1995b], they argued that local observed transition values of the indicators

Paper number 1998JD100075.
0148-0227/99/1998JD100075$09.00

Table 1. New Rate Constants Used for PAN Chemistry

Reaction	Reaction Rate (298.15 K)
ACO3 + NO_2 → PAN	1.37×10^4 ppb^{-1} min^{-1}
PAN → ACO3 + NO_2	2.60×10^{-2} min^{-1}
ACO3 + NO → CH_3O_2 + NO_2	3.54×10^4 ppm^{-1} min^{-1}

can only be applied to assess ozone sensitivities if appropriate criteria have been derived for the local conditions.

This study focuses on the indicator NO_y. The sensitivity of the transition value of NO_y to variations in emissions, temperature, humidity, and radiation is studied using a box model version of Regional Acid Deposition Model (RADM2) [*Stockwell et al.*, 1990]. In a second step the influence of vertical mixing and deposition on the relation of ozone and NO_y is investigated by evaluating the results of one-dimensional simulations. Finally, the transport process of advection is also taken into account. For this purpose, the results of three-dimensional (3-D) simulations and observations are used. To make the individual results of the box model, one-dimensional, and three-dimensional simulations and observations comparable, a normalization procedure is introduced. The investigation is mostly restricted to O_3 in the polluted planetary boundary layer.

2. High- and Low-NO_x Chemistry

The first concepts for reduction of tropospheric ozone in the planetary boundary layer were based on sensitivity analysis of numerical trajectory models by variation of the emissions of NO_x and VOCs for daily ozone maxima. The radical budget was investigated, for example, by examining the sources and sinks of odd hydrogen radicals [*Kleinman*, 1986; *Sillman*, 1991], yielding the definition of high- NO_x when the termination of the radical chain reaction is dominated by

(R1) $$NO_2 + OH \rightarrow HNO_3,$$

(R2) $$NO_2 + CH_3CO_3 \rightarrow PAN$$

and low NO_x when the termination is dominated by

(R3) $$2HO_2 \rightarrow H_2O_2,$$

(R4) $$HO_2 + RO_2 \rightarrow ROOH$$

and the transition regime when (R1)–(R4) are equally important (RO_2 are organic peroxy radicals, and ROOH are organic peroxides). The low-NO_x case is related to increasing ozone as NO_x increases and shows almost insensitivity toward organic compounds. The high-NO_x case is associated with decreasing ozone as NO_x increases and increasing ozone as organic compounds increase [*Sillman et al.*, 1990; *Sillman*, 1995b].

A further approach was published by *Kleinman* [1991, 1994]. He bases his criterion on the relative magnitudes of the rate of radical production (S) and the emission rate of NO_x (E_{NOx}). He found $S > E_{NOx}$ for low-NO_x conditions and $S < E_{NOx}$ for high-NO_x conditions. In the low NO_x state the emitted NO_x is removed quickly because there is an excess of free radicals. In the high-NO_x state the oxidation capacity is not sufficient to remove all NO_x, and the concentration of NO_x will increase if no other removal processes (like deposition) exist. It should be mentioned that in this definition there is not a direct relation to the ozone production.

Zimmermann and Poppe [1993] also investigated the bifurcation of photochemistry controlled by the strength of the source of NO. They used a simplified reaction system which concentrates on generic aspects of the coupling of HO_x and NO_x and found an analytic expression for the transition from one state to the other which is in accordance with Kleinman's result. In the following, the O_3-NO_y relationship considering high- and low-NO_x chemistry is investigated.

3. Sensitivity Studies With a Box Model

As a first step, box model runs with RADM2 [*Stockwell et al.*, 1990] are carried out to study both the basic O_3-NO_y relation which is given by chemical reactions and the sensitivity of the transition value of NO_y. Considering the results of the box model simulations, the influence of transport and deposition processes and effects, which are caused by the spatial and temporal variation of the biogenic and anthropogenic emissions, are excluded. The equation, which governs the development of the concentration c_i of species i with respect to time, is therefore

$$\frac{\partial c_i}{\partial t} = P_i - L_i + E_i, \tag{1}$$

where P_i is the chemical production, L_i is the chemical loss, and E_i is the emission of species i. The RADM2 mechanism takes into account 158 reactions of 63 different species. Updates of the original RADM2 chemistry were made concerning the rate constants of the PAN chemistry [*Stockwell and Kley*, 1994]. The new rate constants are given in Table 1. The initial concentrations were chosen to be those of the PLUME1 case of a chemical model intercomparison [*Kuhn et al.*, 1998]. The PLUME1 case was designed to represent the chemistry in the moderately polluted air of the planetary boundary layer. Diurnal cycles of the photolysis rate coefficients typical for central European summer conditions are prescribed. Table 2 gives the initial concentrations and the ambient conditions. Emissions are included which are representative for European air. Their source strengths are kept constant with time. The simulations are started at noon. Details of the prescribed photolysis rate coefficients and the emissions are given by *Kuhn et al.* [1998].

The RADM2 chemistry conserves total nitrogen. Since no deposition and no other sink of NO_y are included in the box

Table 2. Initial Concentrations and Ambient Conditions for the Box Model Runs

	Dimension	Value
T	[K]	288.15
p	[hPa]	1013.25
N	[cm^{-3}]	2.55×10^{19}
H_2O	[% v/v]	1
O_3	[ppb]	50
NO	[ppb]	0.2
NO_2	[ppb]	0.5
HNO_3	[ppb]	0.1
CO	[ppb]	200
CH_4	[ppb]	1700
Isoprene	[ppb]	0
H_2O_2	[ppb]	2
HCHO	[ppb]	1

model, the concentration of NO_y as a function of time is given by

$$NO_y(t) = NO_y(0) + \int_0^t fE_{NO}\, dt' \qquad (2)$$

E_{NO} is the emission rate of nitrogen oxide, and f is a constant factor and is equal to one for the base case run. Table 3 gives the emissions of the base case run.

The simulations are repeated with different values of f (f = 0.01, 0.1, 0.5, 1, 2, 2.25, 2.5, 2.75, 3, 3.25, 3.5, 3.75, 4, 5, 6, 7, 8, 10) to simulate different VOC/NO_x ratios. Figure 1 shows the temporal development of the ozone concentration for $f = 1$, $f = 2.5$, $f = 5$, and $f = 7$. Starting with the base case run, the ozone concentration increases when $f = 2.5$; that is, when more NO is emitted. At $f = 5$ the ozone concentration is lower than in the base case run, and it even decreases from day to day when $f = 7$. This behavior is well known, and it demonstrates the nonlinearity of photochemistry. For a further evaluation the following procedure is applied to reduce the data. The maximum ozone concentration for each of the simulated days and emission scenarios is plotted versus the corresponding NO_y concentration.

The results of this procedure are shown in Figure 2. For each day starting with low NO_y the ozone concentration increases with increasing NO emissions. This holds up to a certain value of NO_y which shall be defined as the transition value $NO_{y,t}$ with its corresponding ozone concentration $O_{3,t}$. If the emissions are increased further, the maximum ozone concentration decreases again. For a specific day it is obvious that a reduction of NO emissions leads to decreasing ozone concentrations if the NO_y concentration is below the transition value and the contrary behavior if it is beyond the transition value. When NO_y is below the transition value, we call it low-NO_x conditions, and when NO_y is above the transition value, we call it high-NO_x conditions. Since the transition value differs from day to day, it is clear that no universal transition value of NO_y exists.

The following sensitivity studies will concentrate on the results for day 2. On this day the maximum ozone levels are comparable to those which are usually observed over central Europe. For day 2 a transition value of about 26 ppb ($O_{3,t}$ = 135 ppb) is determined.

Table 3. Emissions for the Base Case Run (Box Model)

Species	Chemical Formula	Model Representation	Emissions, ppb/min
Sulfur dioxide	SO_2	SO2	5.20×10^{-4}
Nitrogen oxide	NO	NO	2.60×10^{-3}
Carbon monoxide	CO	CO	5.70×10^{-3}
Acetaldehyde	$C_nH_{2n+1}CHO$	ALD	3.60×10^{-5}
Formaldehyde	HCHO	HCHO	1.40×10^{-4}
C3-C5 alkane	C_3H_8, C_4H_{10}	HC3	2.80×10^{-3}
C6-C8 alkane	C_7H_{16}	HC5	7.90×10^{-4}
Other alkanes ($n \geq 10$)	C_nH_{2n+2}	HC8	4.70×10^{-4}
Ethane	C_2H_6	ETH	2.40×10^{-4}
Ethene	C_2H_4	OL2	4.60×10^{-4}
Terminal alkenes	C_3H_6	OLT	2.30×10^{-4}
Internal alkenes	C_4H_8	OLI	1.80×10^{-4}
Toluene	$C_6H_5CH_3$	TOL	6.60×10^{-4}
Xylene	$C_6H_4(CH_3)_2$	XYL	5.20×10^{-4}
Ketones	CH_3COCH_3	KET	4.40×10^{-4}

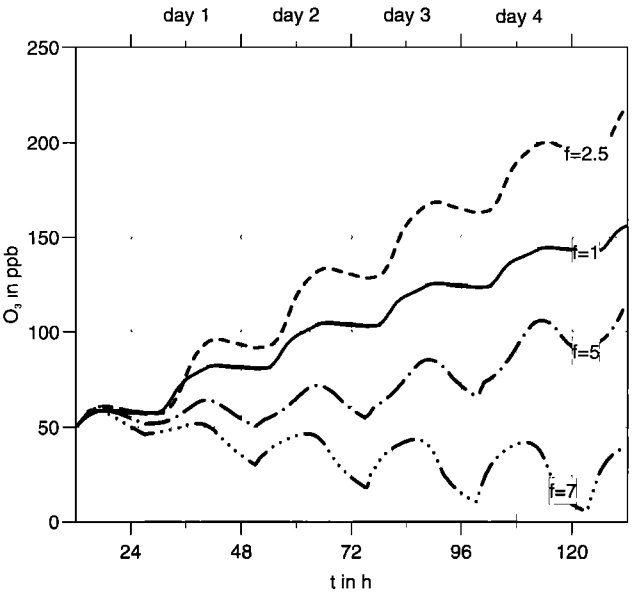

Figure 1. Diurnal cycles of ozone for different NO emission rates. The simulations are started at noon.

In order to study the chemistry in more detail, Figure 3 shows the results for some other species. Although Figure 3 gives only the results of day 2, the principle behavior on the other days is quite similar.

When NO_y is low, that is, at low NO emissions, the oxidizing

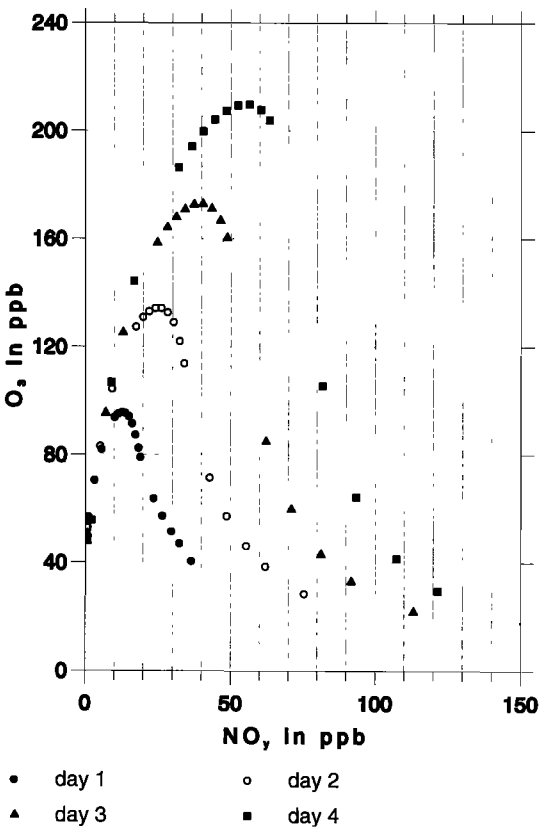

Figure 2. Maximum ozone concentration at different NO_y levels for different days.

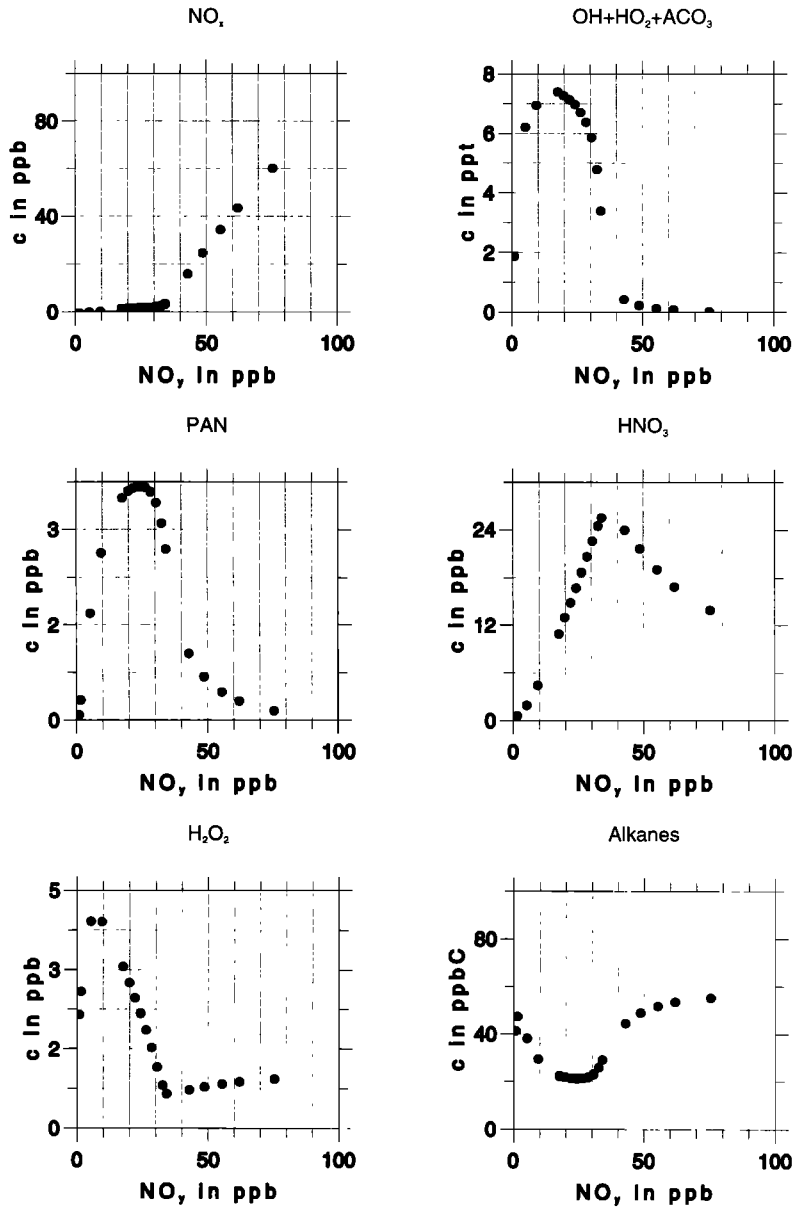

Figure 3. Concentrations of several species at different levels of NO_y for day 2.

potential of the system is high. In this case, nitrogen oxides are quickly removed from the atmosphere and are transformed to other nitrogen species. This results in low concentrations of nitrogen oxides. When NO_y is above 35 ppb, the system becomes saturated with nitrogen oxides, and the supply of radicals declines. The concentration of nitrogen oxides increases linearly with NO_y. At this particular value (NO_y = 35 ppb) the Kleinman criteria holds; that is, $S = E_{NOx}$. It is obvious that this value is higher than the transition value according to our definition.

The concentrations of OH, HO_2, and the acetyl peroxy radical (ACO3) are summed to show the behavior of the main radicals at different levels of NO_y. As mentioned before, there is a high amount of radicals at low NO_y, that is, when the emissions of nitrogen oxides are low. At the same point where the nitrogen oxides start to increase linearly with NO_y there is a sharp decrease in the concentration of radicals. When the concentration of radicals tends to zero, the NO_x-HO_x cycles are decoupled.

PAN, which is formed from NO_2 and the acetyl peroxy radical, shows a similar behavior to ozone. It reaches its maximum when acetyl peroxy radicals are still abundant and NO_2 has a rather high level. At high NO concentrations the acetyl peroxy radical reacts with NO instead of NO_2. Moreover, the supply of acetyl peroxy radical declines. The production of PAN therefore becomes less effective.

The production of HNO_3, which is an important component of NO_y, depends on the concentrations of OH and NO_2. Therefore HNO_3 increases with increasing NO emissions (i.e., with increasing NO_y). For NO_y above 35 ppb, HNO_3 decreases again (although NO_2 increases) because of the decaying supply of OH radicals.

H_2O_2 is produced by the reaction of two HO_2 radicals. This reaction is very efficient as long as the concentration of nitrogen oxides is low. At low emission rates of NO (i.e., low NO_y), high concentrations of H_2O_2 are found.

The alkanes show a local minimum when ozone reaches its

maximum. At this point the reactions with the OH radical are very efficient, and therefore the alkanes reach their minimum. A similar behavior is found for the alkenes and the aromatics.

Figure 2 shows already that no single transition value for NO_y exists. It is therefore worthwhile to study in which way the transition value shifts when the VOC emissions are changing and in which way the transition value is modified by the ambient conditions such as radiation, temperature, and humidity.

3.1. Variation of the VOC Emissions

The box model runs with different NO emissions are repeated, but now the emissions of all VOC components are multiplied by a factor of 2. Figure 4a shows the results for these simulations together with those of the base case runs. In cases of low NO_y concentrations the ozone concentrations are somewhat lower than in the base case run. This is caused by the reactions of alkenes with ozone. At higher NO_y concentrations the production of HO_x radicals is enhanced by the higher VOC emissions. The accumulation of NO_x, which hinders the ozone production, is therefore shifted to higher levels of NO_y. As a consequence, higher ozone concentrations are reached. In addition, the transition value of NO_y shifts to higher concentrations (39 ppb instead of 26 ppb), and O_{3t} reaches 167 ppb.

3.2. Variation of the Photolysis Rate Coefficient

Two series of box model runs are carried out to study the influence of the photolysis rate coefficients on the transition value of NO_y. In case J1 all photolysis rate coefficients involved in RADM2 chemistry were reduced by 50%. For case J2 the photolysis rate coefficients are scaled according to a 10% change of the total ozone column (from 350 Dobson units (DU) to 315 DU). The motivation for this calculation is that photosmog episodes are usually accompanied by clear-sky conditions. During such conditions, changes of the total ozone column have the largest influence on the photolysis rate coefficients. A typical day to day change of the total ozone column during summer is of the order of 10% in central Europe [*Deutscher Wetterdienst (DWD)*, 1992]. Table 4 shows the percentage increase of the photolysis rate coefficients caused by the 10% decrease of the total ozone column. Figure 4b shows the results of the base case run and the cases with the changed photolysis rate coefficients. Since all photolysis rate coefficients are reduced in case J1, the peak ozone concentration is lower than in the base case. The transition value for NO_y is now 17 ppb (O_{3t} = 97 ppb). It was found that in the low-NO_x regime the reduction of the ozone concentration is mainly caused by the changes in the photolysis of NO_2. At higher values of NO_y, especially those photolysis reactions which are producing radicals are important. In case J2 the short wave photolysis rate coefficients are changed. The long wave photolysis rate coefficients are only slightly modified, and the photolysis of NO_2 is totally unchanged. In particular, the effect of the reaction $O_3 + h\nu \rightarrow O_2 + O(^1D)$ becomes important (see Table 4), which is first a sink for ozone, but also a source of radicals. In the low-NO_x regime where we have a surplus of radicals the increasing photolysis of O_3 results in somewhat lower ozone concentrations. When the NO emissions are high, the enhanced production of radicals becomes important, and more ozone is formed. Compared to the base case run, the transition value of NO_y shifts to a higher value in case J2 (28 ppb); however, the peak ozone concentration is only slightly changed.

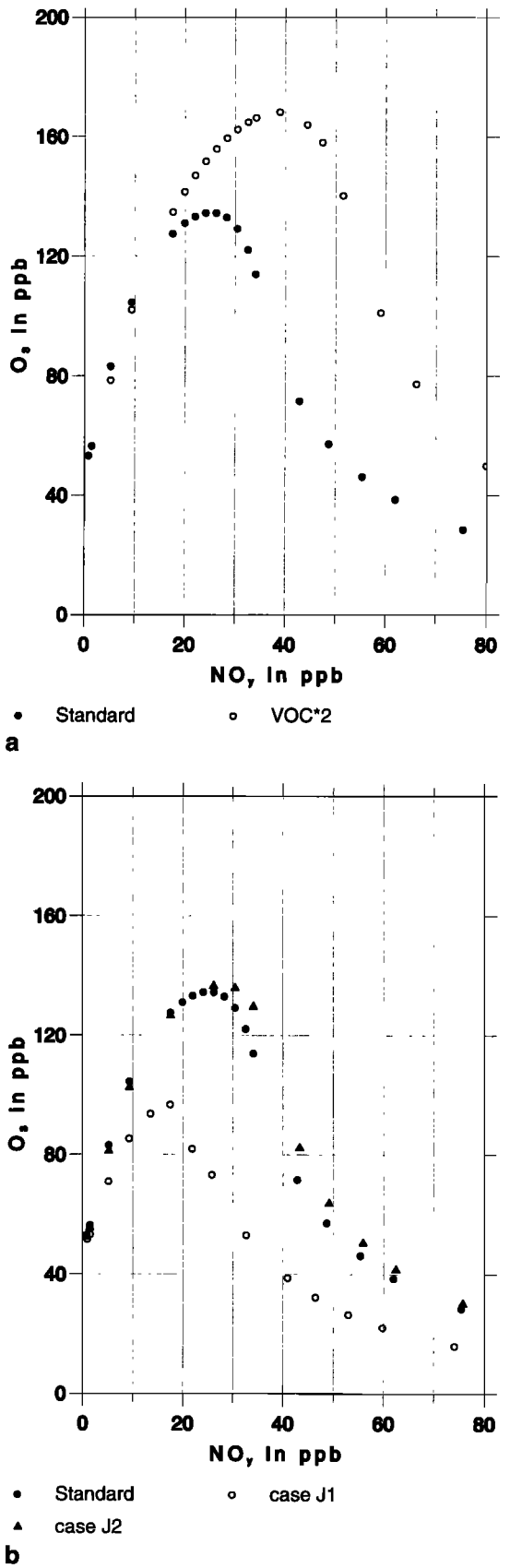

Figure 4. Maximum ozone concentrations at different levels of NO_y for (a) standard and doubled VOC emission rates, (b) different photolysis rate coefficients, (c) different temperature levels, and (d) different water vapor contents.

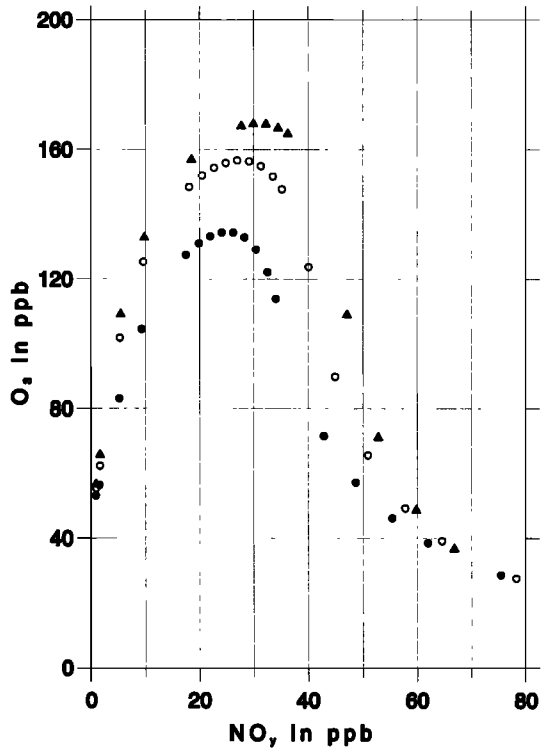

c

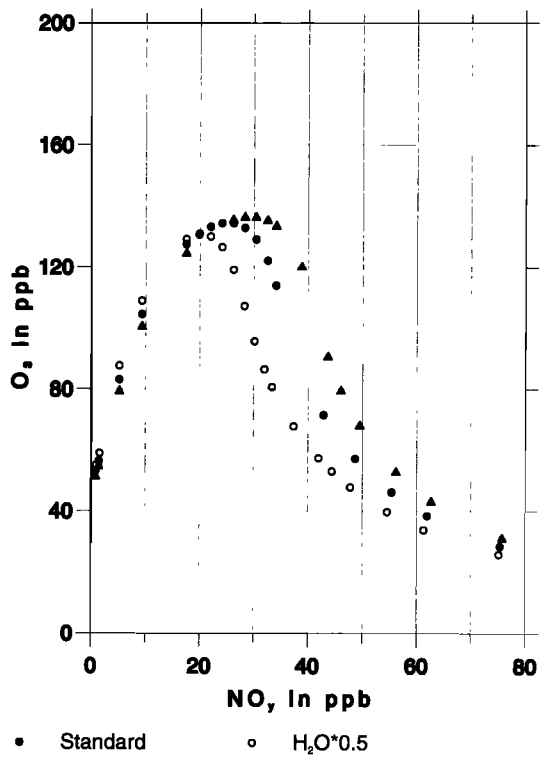

d

Figure 4. (continued)

3.3. Variation of the Temperature

Observations show that temperature and ozone concentrations are strongly correlated [*Kuntasal and Chang*, 1987; *Vogel*, 1996]. Temperature has an impact on the ozone concentration for several reasons [*Cardelino and Chameides*, 1990; *Vogel et al.*, 1995; *Sillman and Samson*, 1995]. First, the biogenic VOC emissions depend on temperature in a nonlinear way [*Tingey*, 1981]. Second, the chemical reactions are temperature dependent. Third, the anthropogenic emissions are correlated with temperature, although this effect is small. Fourth, temperature is an integral measure of the state of the atmosphere. High temperatures are often connected to anticyclonic conditions, situations of low wind speeds, clear skies, and stagnant air masses.

In order to study the direct influence of changes in temperature on photochemistry, two additional series of box model runs are carried out. Compared to the base case runs, the temperature is increased in steps of 10 K (from 288 to 308 K). All other parameters are left unchanged. Figure 4c shows the results of these simulations. The increase of the temperature leads to an increase of the ozone concentration for almost the whole range of NO_y. Only at very low NO_y concentrations and at NO_y concentrations above 60 ppb (i.e., under heavily polluted conditions) the ozone concentration is insensitive to changes in temperature. It is found that the increase of the ozone concentration is mainly caused by the enhanced thermal decomposition of PAN. The lifetime of PAN is 7 hours at 10°C, and it decreases to 18 min at 30°C. At higher temperatures, PAN releases NO_2 which is bound at lower temperatures. In the low-NO_x case the additional supply of the system with NO_2 fosters the production of ozone. Simulations where the rate constant for the thermal decomposition of PAN was kept constant and only the other thermal rate constants were changed according to the increase of the temperature show that in the low-NO_x case the decomposition of PAN is the only reaction which is responsible for the temperature dependence of ozone

Table 4. Percentage Change of Photolysis Rate Coefficients (Case J2)

Photolysis Reaction	Percentage Change
$O_3 + h\nu \rightarrow O(^1D) + O_2$	21.43
$HNO_3 + h\nu \rightarrow OH + NO_2$	12.77
$CH_3CHO + h\nu \rightarrow CH_3O_2 + HO_2 + CO$	10.00
$CH_3ONO_2 + h\nu \rightarrow 0.2\ CH_3CHO + 0.80\ CH_3COCH_3 + HO_2 + NO_2$	10.00
$CH_3COCH_3 + h\nu \rightarrow CH_3CO_3 + C_2H_5O_2$	7.58
$HNO_4 + h\nu \rightarrow HO_2 + NO_2$	6.92
$HCHO + h\nu \rightarrow HO_2 + HO_2 + CO$	4.94
$CH_3COO_2H + h\nu \rightarrow CH_3O_2 + CO_2 + OH$	3.93
$HCOCH = CHCHO + h\nu \rightarrow 0.98HO_2 + 0.02CH_3CO_3 + H(CO)CH = CHCO_3$	3.91
$H_2O_2 + h\nu \rightarrow OH + OH$	3.86
$CH_3O_2H + h\nu \rightarrow HCHO + HO_2 + OH$	3.61
$C_2H_5O_2H + h\nu \rightarrow CH_3CHO + HO_2 + OH$	3.61
$HCOCHO_2 + h\nu \rightarrow 0.45HCHO + 1.55CO + 0.8HO_2$	3.22
$HCHO + h\nu \rightarrow H_2 + CO$	1.63
$O_3 + h\nu \rightarrow O(^3P) + O_2$	1.12
$NO_3 + h\nu \rightarrow NO + O_2$	0.73
$CH_3COCHO + h\nu \rightarrow CH_3CO_3 + HO_2 + CO$	0.54
$NO_3 + h\nu \rightarrow NO_2 + O(^3P)$	0.37
$HONO + h\nu \rightarrow OH + NO$	0.11
$NO_2 + h\nu \rightarrow O(^3P) + NO$	0
$CHOCHO + h\nu \rightarrow 0.13HCHO + 1.87CO$	0

concentration. In the high-NO_x regime it was not possible to identify a single reaction as responsible for the temperature dependence of ozone concentration. The results show that the increase of the temperature causes an increase of the transition value of NO_y from 26 ppb at 288 K to 30 ppb at 308 K and O_{3t} shifts from 135 to 168 ppb.

3.4. Variation of the Humidity

The concentration of water vapor is in one case decreased from 6.2 to 3.1 g/kg and in another case is increased from 6.2 to 9.3 g/kg to study the influence of humidity on the ozone production and on the transition value of NO_y. At the given temperature of 288 K this is related to a change of the relative humidity from 60 to 30% and from 60 to 90%, respectively. This covers the typical range of relative humidity during summer days in Germany [*Höschele and Kalb*, 1988]. The results of these series of simulations are shown in Figure 4d. When the relative humidity changes from 30 to 90%, it is obvious that the peak ozone concentration increases from 131 to 137 ppb and that the transition value of NO_y is remarkably shifted from 20 to 30 ppb. In the low-NO_x regime the ozone concentrations decrease with increasing humidity. In the high-NO_x regime the ozone concentrations increase remarkably with increasing humidity. In the most extreme case the ozone concentration almost doubles when the relative humidity increases from 30 to 90%. This shows that the humidity has a tremendous influence on the ozone production and on the transition value.

In the following, the behavior for the different regimes is explained. The increase of water vapor enhances the rate of reaction

$$\text{(R5)} \qquad H_2O + O(^1D) \rightarrow 2OH.$$

On the one hand, the reaction of $O(^1D)$, which is formed by photolysis of ozone, with H_2O is a sink for ozone, since this prevents the $O(^1D)$ atom from being quenched to the ground state to form ozone again. On the other hand, reaction (R5) is a radical source. The net effect of the enhancement of this reaction depends on the photochemical state: In the low-NO_x regime the role of reaction (R5) as a sink for ozone is dominating. Therefore the increase of water vapor decreases the ozone concentration. When enough NO_x is available and radicals are scarce (i.e., high NO_y), the increase of the OH radical leads to higher ozone concentrations.

3.5. Summary of the Box Model Runs

The sensitivity studies with the box model have shown that in all cases it was possible to identify a transition value which separates those areas which benefit from a reduction of NO emissions from those areas where a decrease of the NO emission leads to an increase of the ozone concentration. The transition value, however, differs for the individual cases. For day 2 of the base case run a transition value of 26 ppb NO_y is found. An increase of the temperature by 20 K leads to a transition value of 30 ppb. When the water vapor content is changed from 3.1 to 9.3 g/kg the transition value shifts from 20 to 30 ppb. Both changes in the transition value are of the same order as the change which is caused by a doubling of the VOC emissions. Although transport processes were not taken into account, this shows that the ambient conditions have a direct impact on the nonlinearity of ozone chemistry and thus they might influence the design and effectiveness of abatement strategies.

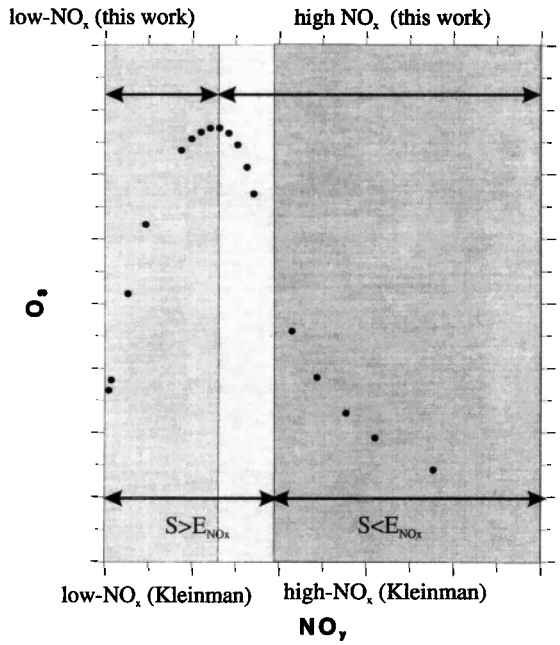

Figure 5. Sketch of Kleinman's and our definitions of low-NO_x and high-NO_x conditions.

3.6. Comparison With Kleinman's Studies

As mentioned above, *Kleinman* [1991] uses the strength of the NO_x source (E_{NOx}) in comparison to the production of radicals (S) to distinguish the two photochemical states. This criterion is to be applied to the box model simulations. For each day of the presented emission scenarios a mean rate of radical production (averaged over 24 hours) is calculated. The production rate of radicals is mainly governed by the reaction of $O(^1D)$ with H_2O and the photolysis of formaldehyde, higher aldehydes, and ketones. In agreement with the results of *Kleinman* [1991], the result for the presented simulations is that in every case the equality between S and E_{NOx} can be found at that value of NO_y where the concentration of radicals drops suddenly down and the NO_x concentration begins to rise. This happens for day 2 in the base case when NO_y equals 35 ppb (Figure 3). However, this value of NO_y is not identical with the transition value related to maximum ozone production because maximum ozone production presupposes the availability of radicals. Therefore the maximum of ozone is located when the radical production is still greater than the emissions of NO_x ($S > E_{NOx}$).

Hence there exists a region where $S > E_{NOx}$ (e.g., low-NO_x conditions according to Kleinman's definition) but where ozone already decreases with increasing NO_x (high-NO_x conditions according to our definition). This was already described by *Sillman* [1995b] and *Kleinman* [1994]. Figure 5 shows that fact schematically. However, for using the NO_y concept in connection with the results of three-dimensional simulations or measurements, it is not practicable to refer to the radical production and the source strength of NO_x because radical production and NO_x emissions can be spatially separated. It therefore remains unclear how to calculate the difference between radical production and NO_x emissions under these circumstances. Moreover, there is no direct relation to the maximum of ozone production and the ozone concentration.

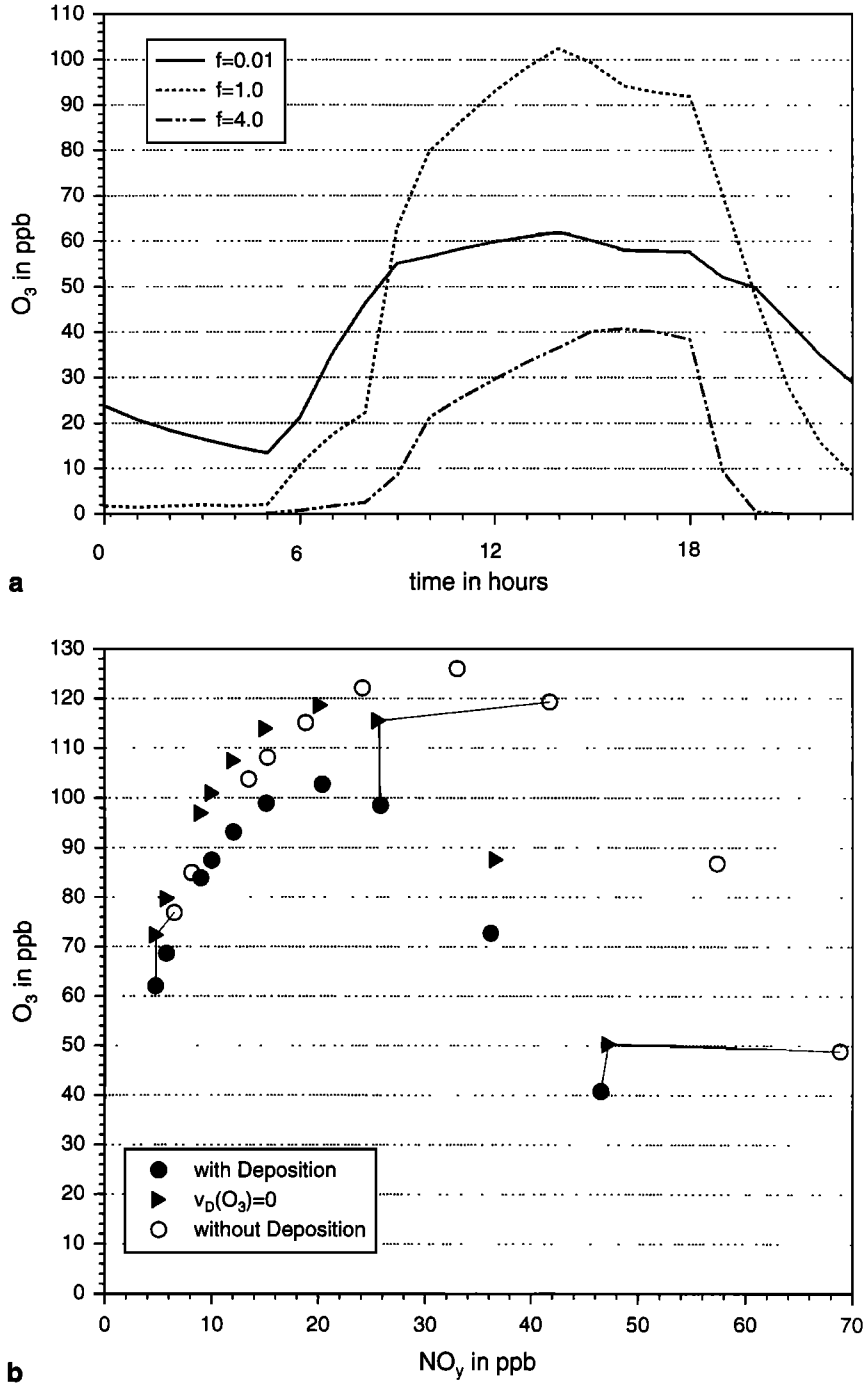

Figure 6. (a) Diurnal cycles of ozone simulated with the one-dimensional model for different NO emissions (f = 0.01, 1.5, 4.0). (b) Ozone concentrations at t = 14 for different NO emissions with and without deposition. The solid lines connect points that belong to the same emission situation.

4. Sensitivity Studies Including Transport and Deposition

In the real atmosphere the concentrations of trace gases are not only controlled by chemistry but also by the interaction of several physical processes. These processes are turbulent diffusion, advection, and deposition. Therefore it is interesting to see if the results found in Section 3 are modified when these processes together with the spatial variability of temperature, humidity, and emissions are taken into account. The different processes and effects are introduced step by step in order to quantify their individual contributions. The numerical simulations are carried out with the comprehensive model system KAMM/DRAIS [*Vogel et al.*, 1995].

4.1. Description of the Model

The model system KAMM/DRAIS uses the nonhydrostatic mesoscale model KAMM [*Adrian and Fiedler*, 1991] as the meteorological driver. It is coupled with a surface vegetation

model developed by *Schaedler* [1989]. This model part gives the lower boundary conditions for temperature and humidity. The submodule DRAIS is used to treat the transport and the diffusion of the reactive trace species. Dry deposition is parameterized using a big leave multiple resistance model [*Baer and Nester*, 1992]. For the treatment of the chemical reactions the RADM2 chemistry is incorporated. The photolysis rate coefficients are determined with the radiation scheme of *Madronich* [1987]. The anthropogenic emissions are precalculated, and the biogenic VOC emissions are calculated depending on the land use, the modeled temperatures, and the modeled radiative fluxes [*McKeen et al.*, 1991b; *Lamb et al.*, 1987; *Vogel et al.*, 1995]. For the parameterization of the NO emissions from the surface a modified scheme of *Yienger and Levy* [1995] is used [*Vogel et al.*, 1996b]. The whole model system runs in a coupled mode. In the vertical direction, 25 layers are used. The vertical grid size varies from 20 m close to the surface up to 400 m at the top of the model domain which is at 8 km above sea level. The time steps, which are used, are of the order of seconds.

4.2. One-Dimensional Model Runs

As a first step, the one-dimensional version of the model system is applied. Compared to the box model runs, vertical diffusion and dry deposition are taken into account as additional processes.

For the concentrations the following equation is solved:

$$\frac{\partial \bar{c}_i}{\partial t} = \frac{\partial}{\partial z} K_{hz} \frac{\partial \bar{c}_i}{\partial z} + \bar{P}_i - \bar{L}_i + E_i \tag{3}$$

K_{hz} is the vertical turbulent diffusion coefficient which is a function of thermal stability and wind shear. Therefore it follows a diurnal cycle and shows a variation with height. The parameter z is the vertical coordinate. At the lower boundary of the atmosphere, dry deposition is used as boundary condition

$$K_{hz} \frac{\partial \bar{c}_i}{\partial z} = -v_{d,i} \bar{c}_i \tag{4}$$

where $v_{d,i}$ is the deposition velocity.

The anthropogenic emissions of NO_x and VOCs for the state of Baden-Württemberg, which is located in the southwestern part of Germany, are available with a spatial resolution of 1×1 km^2 and a temporal resolution of 1 hour [*Obermeier et al.*, 1995]. These data are averaged over the whole domain, and the diurnal cycles of the averaged emissions are used as input data for the one-dimensional model. The biogenic emissions are calculated using the temperature and the photosynthetic active radiation delivered by the meteorological part of the model, taking into account the percentage contribution of the different land use types for the area of Baden-Württemberg. Also, the parameterization of the dry deposition velocities is done according to the percentage contribution of different land use types. A description of the simulated situation, the determination of the emissions, and the deposition velocities are given by *Hammer* [1997]. The results, which are obtained with these emissions, serve as a base case. Similarly to the box model runs, a series of simulations are carried out with the one-dimensional model where the source strength of the anthropogenic NO emissions is multiplied by a factor f (f = 0.01, 0.1, 0.4, 0.5, 0.7, 1.0, 1.5, 2.0, 3.0, 4.0).

Although data are available for 25 vertical layers, we will focus on the results for the first layer above ground (20 m). Figure 6a gives diurnal cycles of ozone for different NO emission strengths for day 2 of the simulation. As expected, the diurnal cycles differ in their minimum and maximum values. There is still some ozone during nighttime when the emissions of NO are low ($f = 0.01$). When the NO emissions are high ($f = 4.0$), the increase of ozone starts very late in the morning, and the maximum ozone concentration is only 40 ppb. The deposition velocity, which is used to parameterize the dry deposition, differs greatly for the individual species involved in photochemistry. During daytime it varies from almost zero for most hydrocarbons, HONO, HNO_4, NO, NO_3, N_2O_5, and CO, up to 3 cm s^{-1} in the case of HNO_3. Around noon we found the following deposition velocities: $v_{d,O_3} \approx 0.7$ cm s^{-1}, $v_{d,PAN} \approx 0.3$ cm s^{-1}, $v_{d,NO_2} \approx 0.5$ cm s^{-1}, $v_{d,HCHO} \approx 0.7$ cm s^{-1}, and $v_{d,aldehydes} \approx 0.5$ cm s^{-1}. It is interesting to compare the lifetime with respect to the deposition process for O_3 and NO_y. For an estimation of the deposition velocity of NO_y the results for $f = 1$ are taken. The deposition velocity for NO_y is approximated by weighting the deposition velocities of the individual components of NO_y with their percentage concentration contribution to NO_y ($HNO_3 \approx 50\%$, PAN $\approx 20\%$, $NO_2 \approx 20\%$, and NO $\approx 10\%$). By this procedure we found a deposition velocity for NO_y of $v_{d,NO_y} \approx 1.66$ cm s^{-1}. Assuming a boundary layer height of 1500 m, deposition as the only relevant process, and no emissions of NO, the lifetime of O_3 would be about 2.5 days, and for NO_y it would be about 1 day. The ratio of the lifetimes of O_3 and NO_y with respect to deposition, however, will depend on the percentage contribution of HNO_3 to total NO_y of any specific situation.

In order to study the role of deposition in more detail, additional sets of simulations are carried out, where in one series the deposition velocities of all species are set equal to zero, whereas in another series only the deposition velocity of ozone is set equal to zero.

Figure 6b shows the O_3-NO_y relation at 20 m aboveground. Data are taken at $t = 14$ hours for each run. A similar pattern to the box model calculations is found. The highest transition value ($NO_{y,t}$ = 33 ppb) and the highest ozone concentrations ($O_{3,t}$ = 126 ppb) are found when the deposition of all species is switched off. The lowest ozone concentration ($O_{3,t}$ = 103 ppb) is found when deposition is taken into account for all species, that is, in the base case. In this case the transition value is $NO_{y,t}$ = 20 ppb. When only the deposition of ozone is switched off, the same transition value as for the base case is found but with higher ozone concentrations as expected ($O_{3,t}$ = 119 ppb).

By comparing the results of the three sets of simulations the effects of deposition of O_3 itself and of deposition of the precursors can be elaborated. They behave differently in the low-NO_x and the high-NO_x regimes. In both regimes, ozone increases when the deposition of ozone is switched off. In the low-NO_x regime, ozone increases when deposition of all species is switched off, whereas in the high-NO_x regime, ozone decreases. The results of these simulations clearly demonstrate the impact of the dry deposition process on the O_3-NO_y relation and especially on the transition value. Deposition of precursors shifts $NO_{y,t}$ to lower values, whereas the deposition of ozone reduces the maximum ozone concentration.

4.3. Three-Dimensional Model Runs

For studying the effects of advection and of the spatial distribution of emissions on the O_3-NO_y relationship, three-

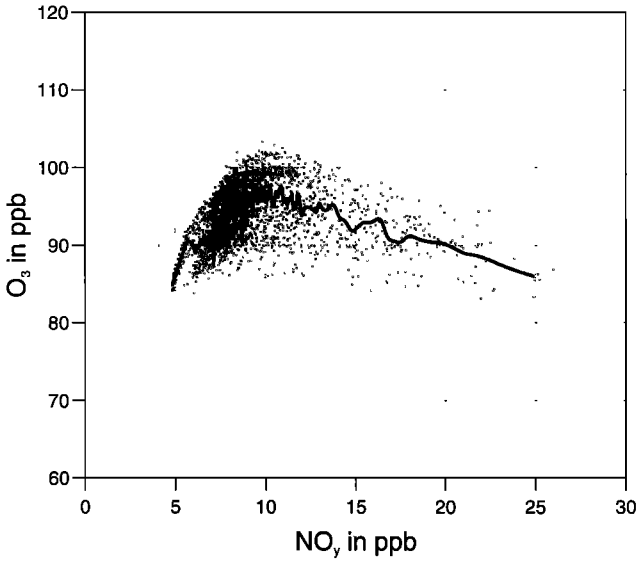

Figure 7. Simulated ozone concentration versus NO_y for August 3, 1990, 1400 CET at 20 m above surface. The thick line gives the data after smoothing.

dimensional simulations are carried out. These simulations come closest to the real situation found in the atmosphere.

For this purpose, the following equation is solved:

$$\frac{\partial \bar{c}_i}{\partial t} = -\bar{u}\frac{\partial \bar{c}_i}{\partial x} - \bar{v}\frac{\partial \bar{c}_i}{\partial y} - \bar{w}\frac{\partial \bar{c}_i}{\partial z} + \frac{\partial}{\partial x}K_{hx}\frac{\partial \bar{c}_i}{\partial x} + \frac{\partial}{\partial y}K_{hy}\frac{\partial \bar{c}_i}{\partial y} + \frac{\partial}{\partial z}K_{hz}\frac{\partial \bar{c}_i}{\partial z} + \bar{P}_i - \bar{L}_i + \bar{E}_i \quad (5)$$

where $\bar{u}$, $\bar{v}$, and $\bar{w}$ are the components of the wind velocity and K_{hx} and K_{hy} are the horizontal turbulent diffusion coefficients. They are all time and space dependent and are calculated at every time step by the meteorological driver of the model system.

A summer smog episode, which occurred at the beginning of August 1990, is simulated to serve as a base case (case A). The model domain covers an area of 171 × 159 km^2 in the southwestern part of Germany and includes the cities of Mannheim, Karlsruhe, and Stuttgart. For the applications presented here the horizontal grid size is 3 km. The time steps are of the order of seconds. The anthropogenic emissions are precalculated with a temporal resolution of 1 hour and a spatial resolution of 1 × 1 km^2 [*Obermeier et al.*, 1995]. During the episode, high temperatures up to 34°C were observed in the area of interest, and it was found that during that situation the amount of biogenic VOC emissions (isoprene plus monoterpenes) was almost the same as the anthropogenic VOC emissions. The maximum ozone concentrations were of the order of 110 ppb. A detailed description of the model system, the model domain, the simulated situation, and the comparison with observations is given by *Vogel et al.* [1995]. Figure 7 shows the correlation of ozone and NO_y at 1400 central European time (CET) on August 3, 1990, for case A. The data are taken from 2637 grid points at 20 m above the surface. As expected, much scatter exists. This scatter is caused by the spatial variation of the emissions and by the three-dimensional distribution of temperature and humidity and the processes of deposition, transport, and turbulent diffusion. In order to reduce the scatter of these data, a smoothing procedure with three grid points and 100 cycles is used. The smoothing starts with K data points $([NO_y],[O_3])_k$. These data points are reordered with respect to $[NO_y]$ to fulfill the relation $[NO_y]_{k-1} < [NO_y]_k$, $k = 2, K$. After reordering, the following smoothing operator is applied to $[NO_y]_k$ and the corresponding $[O_3]_k$:

$$\bar{y}_k = 1/3(y_{k-1} + y_k + y_{k+1})$$
$$\bar{y}_1 = 1/2(y_1 + y_2) \quad (6)$$
$$\bar{y}_K = 1/2(y_{K-1} + y_K)$$

The smoothing is repeated 100 times. By this iteration the number of data points is kept constant.

The thick line in Figure 7 gives the result of this smoothing procedure for the data of case A. The shape of the curve is similar to those of the box model and the one-dimensional runs. For this curve a transition value of $NO_{y,t} = 10.82$ ppb is found.

In addition to the base case run (A), several sensitivity runs with KAMM/DRAIS are carried out for August 3, 1990. A short outline of the sensitivity runs is given in Table 5. In cases B and C the anthropogenic emissions of NO_x and VOC are reduced by 50%. In case D the biogenic and in case E the anthropogenic VOC emissions are switched off. For case F only the biogenic emissions of NO and VOC are taken into account. The initial concentrations of the VOCs for case E are set equal to zero. In case F (only biogenic emissions) the initial concentrations of the precursors of ozone (with the exception

Table 5. Scenarios for the Three-Dimensional Sensitivity Studies

Case	Scenario	$NO_{y,t}$, ppb	$O_{3,t}$, ppb
A	scenario 1990	10.82	97.51
B	scenario 1990 with 50% reduced NO_x emissions	5.90	89.41
C	scenario 1990 with 50% reduced VOC emissions	10.91	95.70
D	scenario 1990 without biogenic VOC emissions	7.91	88.32
E	scenario 1990 without anthropogenic VOC emissions	9.14	80.21
F	only biogenic NO and VOC emissions	NA*	NA*
G	scenario 2000 (emissions of CO, NO_x, VOC reduced by 53, 32, 47%)	8.39	90.61
H	scenario 2000$^+$ (emissions of CO, NO_x, VOC reduced by 70, 43, 61%)	5.98	88.14
I	scenario 2000$^+$ with 50% reduced NO_x emissions	4.36	80.48
J	scenario 2000$^+$ with 50% reduced VOC emissions	6.00	87.75
K	scenario 1990 with homogeneous topography	13.98	112.00
L	scenario 1990 with reduced temperature	9.66	82.23

*NA, not applicable; $NO_{y,t}$ and $O_{3,t}$ are not reached.

of CO) are set equal to zero, and the initial concentration of ozone in the boundary layer is reduced from 85 to 50 ppb. For all other scenarios the initial concentrations of NO_x, VOCs, and ozone are identical to those of case A. Two emission scenarios for the year 2000 were determined [*Obermeier et al.*, 1995]. Scenario 2000 (G) takes into account the emission reductions for CO, NO_x, and VOCs which are caused by such foreseeable technical improvements as increasing use of catalysts and legislative activities in the state of Baden-Württemberg. Scenario 2000^+ (H) includes such additional measures as reduced driving speed and increased use of public transportation units. In the case of scenario 2000 the emissions of CO, NO_x, and VOCs are reduced by 53, 32, and 47%, respectively, while in the case of scenario 2000^+ the emissions of these species are reduced by 70, 43, and 61%, respectively. Additional simulations are carried out for scenario 2000^+ but with a 50% reduction of the NO_x (I) and a 50% reduction of the VOC emissions (J).

The simulations are repeated with the scenario 1990 but with homogeneous terrain height to study the influence of topography on the production of photooxidants (K). For case L the temperature is reduced by 10°C. This has an influence on the chemical reactions (see section 3) and reduces the biogenic VOC emissions by 60%.

The smoothing procedure is applied to the results of each 3-D model run. Figure 8 shows the O_3-NO_y relations after smoothing the data. Table 5 gives the NO_{yt} and O_{3t} values which are obtained for the individual runs.

In the cases of 50% NO_x-emission reduction (B, I) the transition values shift to lower values, and the ozone concentrations decrease. For reduced anthropogenic VOC emissions (C, E, J) the transition values remain unchanged (C, J) or are slightly lower (E). The ozone concentrations are more or less changed depending on the emission situation and on initial concentration profiles. When the biogenic emissions are switched off, the transition value falls from 10.82 ppb (A) to 7.91 ppb (D). This strong decrease of the transition value of NO_y might be caused by the high reactivity of the biogenic VOC emissions. In cases G and H the emissions of NO_x and VOCs are both reduced. In both simulations the transition values of NO_y and the ozone concentrations are lower. When only biogenic emissions are taken into account (F), the ozone concentrations are decreased tremendously. Here the NO_y concentrations do not reach a transition value; that is, the atmosphere is totally in the low-NO_x regime. Case K shows the effect of homogeneous terrain height. It is found that in this case the deposition of ozone and of the precursors of ozone is smaller. The difference is caused by secondary circulation systems (slope and valley wind) that develop in the case of real terrain height during the night [*Uhrner*, 1996]. Compared with the homogeneous terrain height case, these circulation systems enhance the deposition flux during the night hours by up to a factor of 2. Consequently, NO_{yt} increases to 13.98 ppb, and O_{3t} increases to 112 ppb for case K. When the temperature is reduced by 10°C (L), the biogenic VOC emissions are reduced, and as shown in section 3, less ozone is produced by chemical transformation. Both effects lead to less ozone. The transition value of NO_y is slightly lowered.

One can ask if it is justified to reduce the scatter of the data by smoothing and to operate with one single transition value for the whole area. It is certainly not possible to do so if totally different emission conditions are present in a specific area of interest. For example, the data presented by *Trainer et al.*

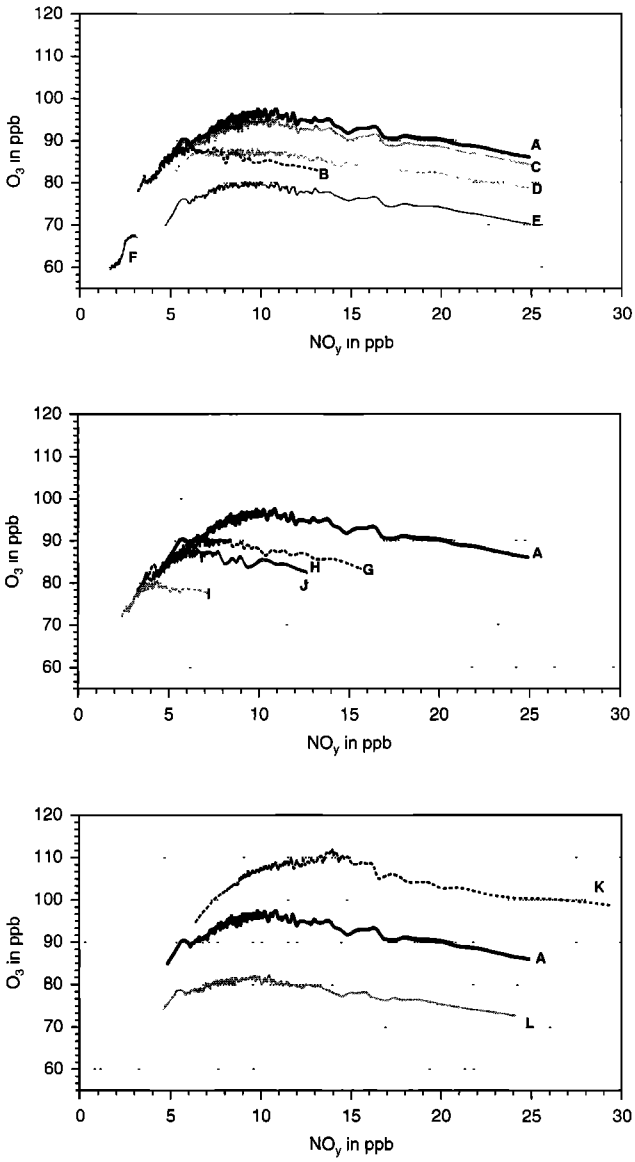

Figure 8. Simulated ozone concentration versus NO_y for the different scenarios after smoothing.

[1995, Figure 6] in the surroundings of Birmingham show two separated plumes. One emerges from a power plant, and another emerges from the city of Birmingham. In such a case a smoothing of data would result in a transition value that is neither valid for the power plant plume nor for the city plume. However, in case of Baden-Württemberg the emissions are rather uniformly distributed over the whole domain, and the plumes emerging from the different source types (highways, power plants, cities) are overlapping each other. In our case a single transition value therefore may be justified.

In order to check if the procedure to determine the transition value could be of practical use for our area of interest, the difference of the ozone concentrations for the base case run and the run with the reduced NO_x emissions (A − B) at 1400 CET is calculated. In addition to ΔO_3, the thick line in Figure 9 shows the 11 ppb NO_y contour line for the base case run. The largest decrease of the ozone concentration is found in areas where the NO_y concentration is below the transition value. The differences are very small in those areas where the NO_y con-

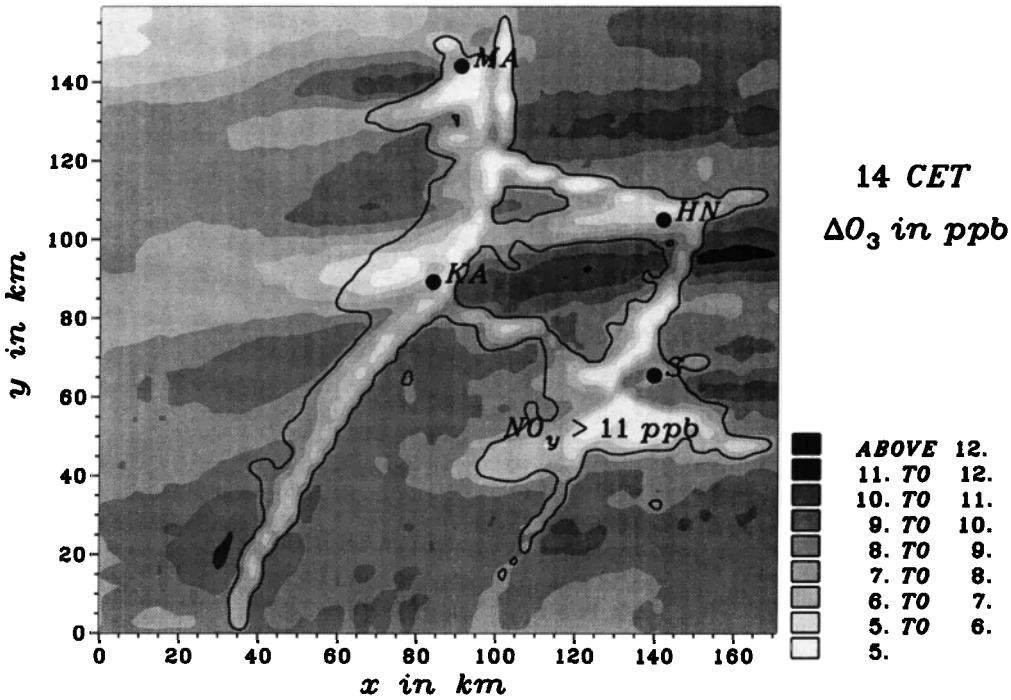

Figure 9. Simulated distribution of ΔO_3 (case A minus case B) for August 3, 1990, 1400 CET at 20 m above surface. The thick contour line gives the 11 ppb NO_y concentration of the base case run (case A).

centration is above the transition value. No increase of the ozone concentration is found, although it could be expected from Figure 7. The reasons for this are advection and diffusion processes. Areas where one might expect an increase of the ozone concentration (high-NO_x conditions) are surrounded by areas where low NO_y is found. In areas where NO_y is below NO_{yt}, ozone is reduced by decreasing NO_x emissions. Therefore lower ozone concentrations are transported into those areas where an increase of the ozone could be expected without transport processes. However, Figure 9 shows also regions where the concept fails. Especially in the lee of Karlsruhe the contours of ΔO_3 and NO_{yt} are crossing. This shows that the transition value determined for the whole model domain by smoothing the individual points is not valid in this specific region. In the major part of the model domain, however, the transition value derived by smoothing separates low-NO_x and high-NO_x conditions.

Another question, which should be answered, is how NO_y is affected by changing the NO_x emissions. In the cases of the box model simulations a direct relation between NO_x emissions and NO_y exists (equation (2)). In the three-dimensional case when deposition is present, it is not clear if such a relation still holds. In our case it is found that a reduction of the NO_x emissions by 50% is indeed connected with an NO_y decrease of almost 50% close to the sources. At larger distances from the sources the decrease of NO_y is only 35%. In case B the relative contribution of HNO_3 to NO_y is smaller than in case A at larger distances from the sources, and hence less NO_y is removed from the atmosphere.

Figure 10 depicts scatterplots of ΔO_3 (A − B, A − C, A − D, A − E) and NO_y for the base case (A) for selected emission reduction scenarios. Individual grid points and average conditions for intervals of 1 ppb of NO_y are shown. It is found that in the case of NO_x reduction (A − B) the highest ozone decrease exists in those areas where NO_y is below the transition value derived from the smoothing procedure of case *A*. The majority of grid points (80%) belong to those areas. No increase of ozone is found above the transition value. As mentioned before, this is caused by transport processes.

In case of VOC emission reductions the largest decrease of ozone is found in those areas where NO_y is above the transition value. The highest ΔO_3 is found when all anthropogenic VOC emissions are switched off (A − E). This can be explained by the fact that in this case the background concentrations are also set equal to zero. The decrease of ozone is lowest when the anthropogenic VOC emissions are reduced by 50% (A − C) because of the high contribution of the biogenic VOC emissions to total VOC emissions.

The results depicted in Figures 9 and 10 show the usefulness and the limitation of the concept of the indicator NO_y. Although the concept holds for large parts of the domain, it fails in those areas where the local O_3-NO_y relation differs significantly from the mean O_3-NO_y relation.

5. Observations

As a next step, observations are looked at to see if some of the typical features obtained with the numerical model are also found in reality. The measurements are taken from the TRACT campaign which took place in September 1992 [*Kossmann et al.*, 1998] in the southwestern part of Germany. The data of one flight, which took place on September 21, 1992, between 1300 and 1600 CET, are analyzed. The area covered by the field campaign includes the model domain presented in Section 4. Figure 11a gives time series of O_3 and NO_y during that flight. The aircraft passed through two intensive plumes which belong to the city of Basel and the city of Mannheim. It moved at an altitude between 600 m above sea level in the area of Mannheim (100 m above sea level) and 1400 m above sea level when it passed the Black Forest and the Vosges moun-

tains. Thus it was always inside the lower boundary layer. Figure 11b shows the correlation of O_3 and NO_y concentrations for that time series. It is obvious that the observed data show the same behavior as the model results (Figure 7). The observations were made late in September, and therefore the photolysis rate coefficients are lower, which should be followed by a lower transition value (see Section 3.2). The maximum temperature on this day was reached in the Rhine Valley and was of the order of 25°C. Compared to the simulated situation, where the temperatures were well above 32°C, this should also lead to a lower transition value. As expected, the transition value found for the observation (NO_{yt} = 7.78 ppb) is indeed lower than for the model results.

For our area of interest we find a general agreement in the behavior of the simulated and observed O_3-NO_y relationship. The scatter in the observed O_3-NO_y data is comparable to the simulated data. A plausible transition value is found that is lower than the simulated one.

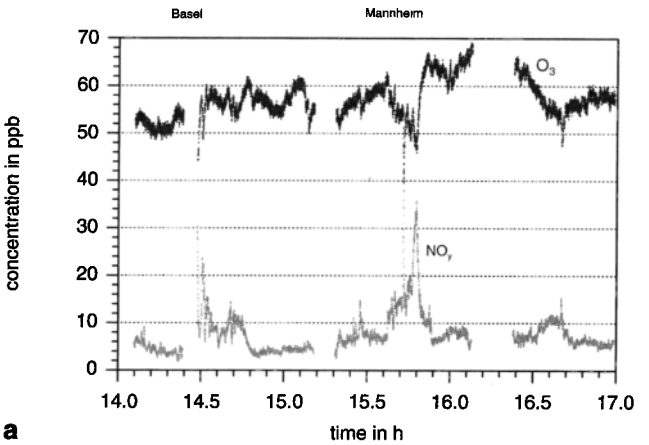

Figure 11a. Time series of measured O_3 and NO_y concentrations during the TRACT campaign on September 21, 1992.

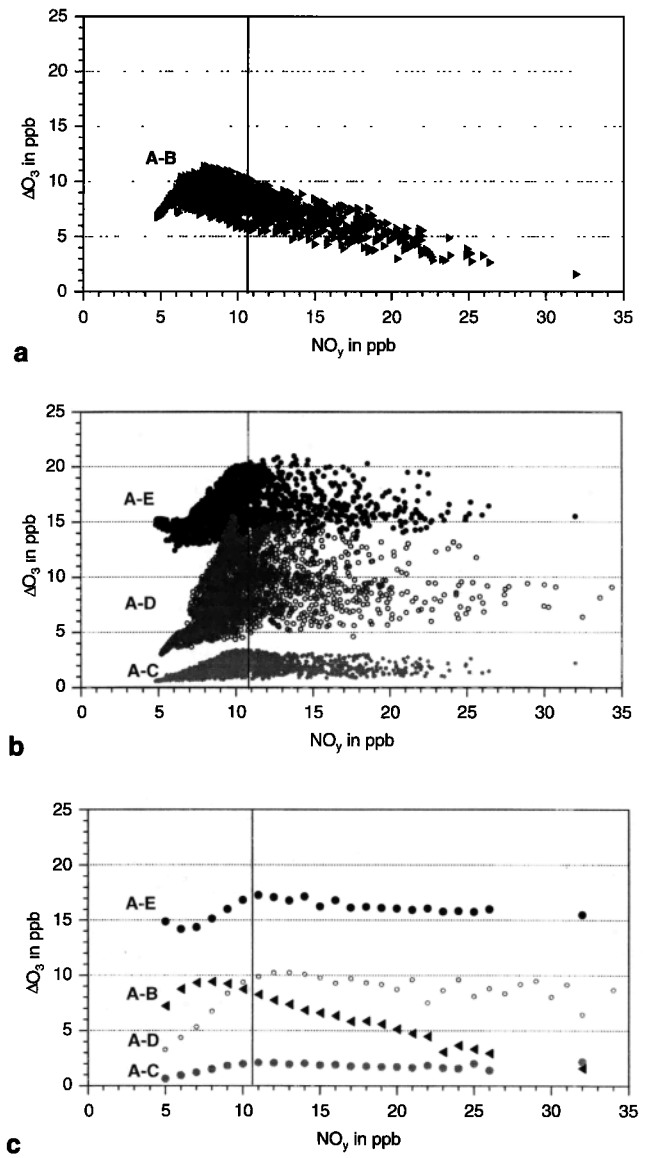

Figure 10. Simulated distribution of ΔO_3 versus NO_y of case A for different emission scenarios at 20 m aboveground. (a and b) Raw data and (c) averaged data for intervals of 1 ppb NO_y.

6. Procedure of Normalization

The results of the box model runs, those of the one-dimensional and three-dimensional simulations, and those of the observations produced similar shapes of the O_3-NO_y relationships. Depending on ambient and emission conditions, the relationships differed in their transition value NO_{yt} and the corresponding ozone concentration O_{3t}. For a better comparison of the results the following normalization procedure is introduced.

$$\langle NO_y \rangle = \frac{[NO_y]}{[NO_{yt}]} \tag{7}$$

$$\langle O_3 \rangle = \frac{[O_3]}{[O_{3t}]} \tag{8}$$

The normalization procedure is applied to each O_3-NO_y relation found in Sections 3, 4, and 5 using the individual O_{3t} and NO_{yt} values (Table 5). This procedure forces all normalized

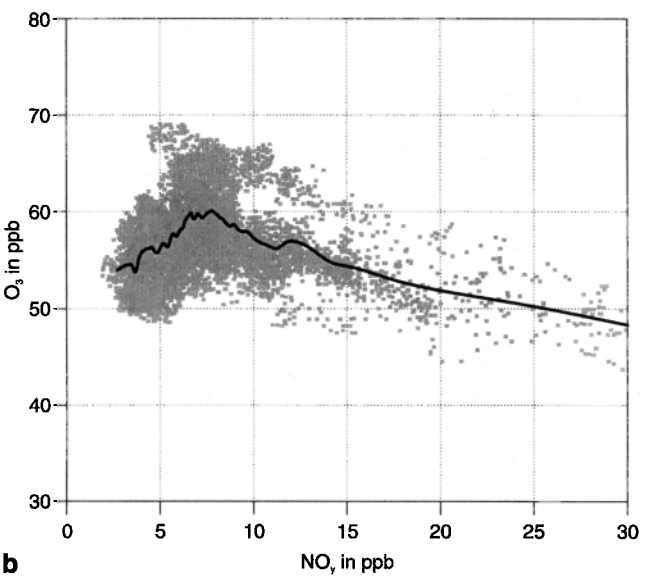

Figure 11b. Measured O_3 concentrations versus measured NO_y concentrations. The thick line gives the data after smoothing.

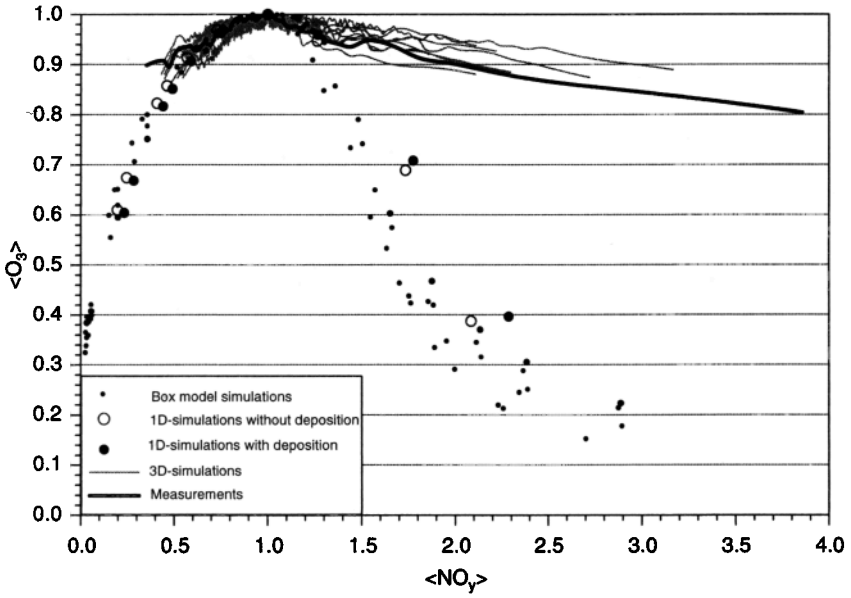

Figure 12. Normalized results of all model simulations and of the TRACT observations.

curves to fall together at $\langle O_3 \rangle = \langle NO_y \rangle = 1$. The results after normalization are presented in Figure 12.

For the box model runs all data fall together within a few percent below $\langle NO_{yt} \rangle = 1$. More detailed analyses of that data show that at $\langle NO_y \rangle \approx 1.5$ the radical production is identical to the emissions of NO_x ($S \approx E_{NO_x}$). This point separates the low-NO_x and high-NO_x conditions according to Kleinman's definition. Above $\langle NO_y \rangle = 1.5$ the scatter of the data becomes larger, but even in that case the data fall together within 10%. Under high-NO_x conditions the availability of radicals becomes important for ozone production and explains the scatter.

When vertical mixing and deposition are taken into account, that is, in the case of the one-dimensional simulations, there is a favorable agreement with the results of the box model runs when $\langle NO_y \rangle$ is less than 1. Above that value the results of the one-dimensional runs and the box model runs differ a little bit more. However, the differences are still small. At a given value of $\langle NO_y \rangle$, higher values of $\langle O_3 \rangle$ are found even in the cases when deposition is switched off. This must be attributed to the additional process of vertical mixing. The reason for this modification is that although much NO is emitted on the ground level, causing a local reduction of ozone, NO is transported to higher levels above ground and is diluted. Ozone forms at higher levels and is mixed downward [*Vogel et al.*, 1992]. This means that by vertical transport we get more ozone in the high-NO_x case than would be the case if only chemical processes were present.

When all relevant processes are taken into account, that is, in the case of the three-dimensional simulations, the following is found. When $\langle NO_y \rangle$ is less than 1, the results are close to those of the box model and the one-dimensional runs. It is not possible to separate the individual contributions of the different processes to the remaining scatter. When $\langle NO_y \rangle$ is above the transition value, the results of the three-dimensional model runs are totally different from those of the box- and the one-dimensional models. The decrease of $\langle O_3 \rangle$ with increasing $\langle NO_y \rangle$ is much steeper in the results of the box model runs than in those of the three-dimensional simulations. The difference is mainly caused by advection and in a smaller amount also by turbulent diffusion. Titration of ozone in the source regions is partly compensated by transport processes. This finding has consequences for abatement strategies. Under high-NO_x conditions the increase of the ozone concentration is less pronounced when the NO_x emissions are reduced than in the case of pure chemistry as described by the box model.

Finally, the measurements are also normalized using equations (7) and (8). The normalized $\langle O_3 \rangle$-$\langle NO_y \rangle$ relation for the TRACT campaign fits very well with the results of the three-dimensional model runs. Similarly to the model results, the observations show lower sensitivity to changes in NO_y under high-NO_x conditions than would be expected in the case of pure chemistry. This confirms our interpretation of the significant role of transport.

7. Summary and Conclusions

This study has focused on NO_y as an indicator for ozone sensitivity in cases of NO_x emission changes. First, a box model was used to study the principle relation of ozone and other trace species to NO_y. In agreement with previous studies, a transition value for NO_y could be identified that separates high-NO_x from low-NO_x conditions. Sensitivity studies with the box model showed that the transition value depends on the VOC emissions, the photolysis rate coefficients, and the water vapor content. The enhanced radical production at higher NO_y concentrations is responsible for the increase in the transition value when these variables were increased. A change in temperature also shifts the transition value.

We compared our transition value which defines the separation of the low-NO_x from the high-NO_x conditions with Kleinman's definitions of the high-NO_x and the low-NO_x states. It was found that the transition of the different regimes does not happen at the same values of NO_y. Our results confirm one advantage of Kleinman's definition of high- and low-NO_x conditions. When $S = E_{NO_x}$, the highest sensitivity of ozone to changes in VOC emissions and ambient conditions occurs. However, the criterion of Kleinman needs the knowl-

edge of the production of radicals to compare it with the emissions of NO. In the atmosphere, and even with a three-dimensional model, it would be hard to identify the local radical production and the corresponding emissions in order to check Kleinman's criterion. Therefore, for practical use, our definition is more convenient to apply.

Sensitivity runs with a one-dimensional model have shown the impact of dry deposition on the O_3-NO_y relationship. When dry deposition was switched off, the transition value of NO_y was shifted to higher values, and an increase in the maximum ozone concentration was found.

The results of three-dimensional simulations with a comprehensive model system were used to test an objective method for the determination of the transition value of NO_y. Although the method was useful to separate high- and low-NO_x regions for a large part of the model domain, limitations were detected. The concept failed in those areas where the local O_3-NO_y relation differs significantly from the mean one.

A number of sensitivity studies were carried out with the three-dimensional model using different emission scenarios and ambient conditions. These sensitivity runs supported the findings of the box model runs; that is, no single transition value was found. The transition values shifted in agreement with the box model runs. It is worthwhile to notice that a decrease in temperature shifted NO_y toward lower values and O_{3t} decreased remarkably. In this case the reduction of ozone was even larger than in the case where NO_x emissions were reduced by 50%. This demonstrates the large impact of temperature on ozone production.

A normalization procedure was introduced and was first applied to the results of the box model runs. For a single simulated day this procedure made the results of all scenarios fall together within a few percent. When the normalization procedure was applied to the results of the three-dimensional model, an agreement with the results of the box model and the one-dimensional model was found in the cases of low-NO_x conditions. Under high-NO_x conditions the decrease of the normalized ozone concentration $\langle O_3 \rangle$ with increasing $\langle NO_y \rangle$ was tremendously less pronounced for the results of the three-dimensional model than for those of the box model. This is caused by transport processes, mainly by advection. The consequence is that under high-NO_x conditions the sensitivity of ozone to changes in NO_y is less than would be expected from pure chemistry.

The normalization procedure was also applied to observations which were made in southwest Germany. When the normalized observations were compared with the results of the three-dimensional simulations, the agreement was good. With respect to NO_x abatement strategies, our findings allow the following conclusions. The maximum ozone concentration, which can be reached for our area, is determined by the emission situation and the ambient conditions. If we want to reduce this maximum value by reducing NO_x emissions, the benefit is rather small as long as the reductions are less than 50%. Nevertheless, for the major part of Baden-Württemberg, low-NO_x conditions apply. Consequently, NO_x abatement strategies would be favored instead of VOC abatement strategies.

Acknowledgments. We acknowledge the valuable comments of two anonymous reviewers on an earlier version of this paper. We thank Sandy Sillman for several useful discussions via e-mail.

References

Adrian, G., and F. Fiedler, Simulation of unstationary wind and temperature fields over complex terrain and comparison with observation, *Contrib. Atmos. Phys.*, *64*(1), 27–48, 1991.

Andreani-Aksoyoglu, S., and J. Keller, Indicator species for O_3 sensitivity relative to NO_x and VOC in Switzerland and their dependence on meteorology, in *Air Pollution V Modelling, Monitoring and Management*, edited by H. Power, T. Tirabassi, and C. A. Brebbia, pp. 883–891, Comput. Mech., Billerica, Mass., 1997.

Atkinson, R., Kinetics and mechanisms of the gas phase reactions of the hydroxyl radical with organic compounds under atmospheric conditions, *Chem. Rev.*, *86*, 169–201, 1986.

Baer, M., and K. Nester, Parametrization of trace gas deposition velocities for a regional mesoscale diffusion model, *Ann. Geophys.*, *10*, 912–923, 1992.

Cardelino, C. A., and W. L. Chameides, Natural hydrocarbons, urbanization, and urban ozone, *J. Geophys. Res.*, *95*, 13,971–13,979, 1990.

Deutscher Wetterdienst (DWD), Meterorologisches Observatorium Hohenpeissenberg, Sonderbeobachtungen: Ergebnisse der aerologischen und bodennahen Ozonmessungen im ersten Halbjahr 1991, *Nr. 65*, Hohenpeissenberg, 1992.

Hammer, M., Numerische Simulationen zum Einfluß lang- und kurzfristiger Änderungen der Witterungs- und Emissionsverhältnisse auf das troposphärische Ozon, Diplomarbeit, Inst. für Meteorol. und Klimaforsch., Univ. Karlsruhe/Forsch. Karlsruhe, Karlsruhe, Germany, 1997.

Höschele, K., and M. Kalb, Das Klima ausgewählter Orte der Bundesrepublik Deutschland Karlsruhe, Berichte des Deutschen Wetterdienstes, *Nr. 174*, Offenbach am Main, Germany, 1988.

Kleinman, L. I., Photochemical formation of peroxides in the boundary layer, *J. Geophys. Res.*, *91*, 10,889–10,904, 1986.

Kleinman, L. I., Seasonal dependence of boundary layer peroxide concentration: The low and high NO_x regimes, *J. Geophys. Res.*, *96*, 20,721–20,733, 1991.

Kleinman, L. I., Low and high NO_x tropospheric photochemistry, *J. Geophys. Res.*, *99*, 16,831–16,838, 1994.

Kossmann, M., R. Vögtlin, U. Corsmeier, B. Vogel, F. Fiedler, H. J. Binder, N. Kalthoff, and F. Beyrich, Aspects of the convective boundary layer structure over complex terrain, *Atmos. Environ.*, *32*, 1323–1348, 1998.

Kuhn, M., et al., Intercomparison of the gas phase chemistry in several chemistry and transport models, *Atmos. Environ.*, *32*, 693–709, 1998.

Kuntasal, G., and T. J. Chang, Trends and relationships of O_3, NO_x, and HC in the south coast air basin of California, *J. Air Pollut. Control Assoc.*, *37*, 1158–1163, 1987.

Lamb, B., A. Guenther, D. Gay, and H. Westberg, A national inventory of biogenic hydrocarbon emissions, *Atmos. Environ.*, *21*, 1695–1705, 1987.

Lu, C.-H., and J. S. Chang, On the indicator-based approach to asses ozone sensitivities to reductions in VOC and NO_x emissions, in *Air Pollution V Modelling, Monitoring and Management*, edited by H. Power, T. Tirabassi, and C. A. Brebbia, pp. 913–922, Comput. Mech., Billerica, Mass., 1997.

Madronich, S., Intercomparison of NO_2 photodissociation and UV radiometer measurements, *Atmos. Environ.*, *21*, 569–578, 1987.

McKeen, S. A., E.-Y. Hsie, M. Trainer, R. Tallamraju, and S. Liu, A regional model study of the ozone budget in the eastern United States, *J. Geophys. Res.*, *96*, 10,809–10,845, 1991a.

McKeen, S. A., E.-Y. Hsie, and S. C. Liu, A study of the dependence of rural ozone on ozone precursors in the eastern United States, *J. Geophys. Res.*, *96*, 15,377–15,394, 1991b.

Milford, J. B., D. Gao, S. Sillman, P. Blossey, and A. G. Russel, Total reactive nitrogen (NO_y) as an indicator of the sensitivity of ozone to reductions in hydrocarbon and NO_x emissions, *J. Geophys. Res.*, *99*, 3533–3542, 1994.

Morris, R. E., and T. C. Myers, Users guide for the urban airshed model, *Rep. EPA-450/4-90-007A*, U.S. Environ. Prot. Agency, Washington, D. C., 1990.

National Research Council (NRC), Committee on Tropospheric Ozone Formation, in *Rethinking the Ozone Problem in Urban and Regional Air Pollution*, Natl. Acad. Press, Washington, D. C., 1991.

Obermeier, A., R. Friedrich, C. John, J. Seier, H. Vogel, F. Fiedler, and B. Vogel, Photosmog, Möglichkeiten und Strategien zur Emissionsminderung, Ecomed, Landsberg, Germany, 1995.

Schaedler, G., Triggering of atmospheric circulations by moisture in-

homogeneities of the Earth's surface, *Boundary Layer Meteorol., 51*, 1–29, 1989.

Seinfeld, J. H., *Atmospheric Chemistry and Physics of Air Pollution*, John Wiley, New York, 1986.

Sillman, S., A numerical solution to the equations of tropospheric chemistry based on an analysis of sources and sinks of odd hydrogen, *J. Geophys. Res., 96*, 20,735–20,744, 1991.

Sillman, S., New developments in understanding the relation between ozone, NO_x and hydrocarbons in urban atmospheres, in *Progress and Problems in Atmospheric Chemistry Adv. Ser. Phys. Chem.*, vol. 3, edited by J. R. Barker, pp. 145–171, World Sci., River Edge, N. J., 1995a.

Sillman, S., The use of NO_y, H_2O_2, and HNO_3 as indicator for the NO_x-hydrocarbon sensitivity in urban locations, *J. Geophys. Res., 100*, 14,175–14,188, 1995b.

Sillman, S., and P. J. Samson, Impact of temperature on oxidant photochemistry in urban, polluted rural, and remote environments, *J. Geophys. Res., 100*, 11,497–11,508, 1995.

Sillman, S., J. A. Logan, and S. C. Wofsy, The sensitivity of ozone to nitrogen oxides and hydrocarbons in regional ozone episodes, *J. Geophys. Res., 95*, 1837–1851, 1990.

Staffelbach, T., and A. Neftel, Photochemical oxidant formation over southern Switzerland, 2, Model results, *J. Geophys. Res., 102*, 23,363–23,373, 1997.

Staffelbach, T., et al., Photochemical oxidant formation over southern Switzerland, 1, Results from summer 1994, *J. Geophys. Res., 102*, 23,345–23,362, 1997.

Stockwell, B. W., and D. Kley, The Euro-RADM mechanism: A gas-phase chemical mechanism for European air quality studies, Forsch. Jülich GmbH (KFA), Jülich, Germany, 1994.

Stockwell, B. W., P. Middleton, J. S. Chang, and X. Tang, The second-generation regional acid deposition model chemical mechanism for regional air quality modeling, *J. Geophys. Res., 95*, 16,343–16,368, 1990.

Tingey, D. T., The effect of environmental factors on the emission of biogenic hydrocarbons from live oak and slash pine, in *Atmospheric Biogenic Hydrocarbons*, vol. 1, edited by J. J. Bufalini and R. R. Arnts, pp. 53–79, Butterworth-Heinemann, Newton, Mass., 1981.

Trainer, M., B. A. Ridley, M. P. Buhr, G. Kok, J. Walega, G. Hübler, D. D. Parrish, and F. C. Fehsenfeld, Regional ozone and urban plumes in the southeastern United States: Birmingham, a case study, *J. Geophys. Res., 100*, 18,823–18,834, 1995.

Uhrner, U., Physikalische Ursachen regionaler Unterschiede in der nächtlichen Ozonverteilung, Diplomarbeit, Univ. Karlsruhe/Forsch. Karlsruhe, Karlsruhe, Germany, 1996.

Vogel, B., The effect of climate change during the last 120 years on the ozone concentration in the south-western part of Germany, in *Proceedings of EUROTRAC Symposium '96*, edited by P. M. Borrell et al., pp. 939–942, Comput. Mech., Billerica, Mass., 1996.

Vogel, B., H. Vogel, and F. Fiedler, Numerical simulation of the interaction of transport, diffusion and chemical reactions in an urban plume, *NASA Conf. Publ., 3266*, pp. 97–100, 1992.

Vogel, B., F. Fiedler, and H. Vogel, Influence of topography and biogenic volatile organic compounds emissions in the state of Baden-Württemberg on ozone concentrations during episodes of high air temperatures, *J. Geophys. Res., 100*, 22,907–22,928, 1995.

Vogel, B., F. Fiedler, and H. Vogel, NO_y as an indicator species for ozone sensitivity to emission reductions, in *Proceedings of EUROTRAC Symposium '96*, edited by P. M. Borrell et al., pp. 757–760, Comput. Mech., Billerica, Mass., 1996a.

Vogel, B., F. Fiedler, and H. Vogel, Untersuchungen zum Einfluß biogener Stickoxid- und Kohlenwasserstoffemissionen auf die Ozonverteilung im regionalen Bereich, Annalen der Meteorologie, Deutscher Wetterdienst, pp. 184–185, Offenbach, Germany, 1996b.

Yienger, J. J., and H. Levy II, Empirical model of global soil-biogenic NO_x emissions, *J. Geophys. Res., 100*, 11,447–11,464, 1995.

Zimmermann, H., Field phase report of the TRACT field measurement campaign, EUROTRAC, Int. Sci. Secr., Garmisch-Partenkirchen, Germany, 1995.

Zimmermann, J., and D. Poppe, Nonlinear chemical couplings in the NO_x-HO_x gas phase chemistry, *J. Atmos. Chem., 17*, 141–155, 1993.

F. Fiedler, N. Riemer, B. Vogel, and H. Vogel, Institut fur Meteorologie und Klimaforschung, Forschungszentrum Karlsruhe, Universität Karlsruhe, Postfach 3640, 76021 Karlsruhe, Germany. (e-mail: bernhard.vogel@imk.fzk.de)

(Received August 11, 1998; revised November 5, 1998; accepted November 10, 1998.)